

Conserved tyrosine kinase promotes the import of silencing RNA into *Caenorhabditis elegans* cells

Antony M. Jose^{1,2}, Yunsoo A. Kim¹, Steven Leal-Ekman, and Craig P. Hunter³

Department of Molecular and Cellular Biology, Harvard University, Cambridge, MA 02138

Edited by Iva Greenwald, Columbia University, New York, NY, and approved July 26, 2012 (received for review January 23, 2012)

RNA silencing in *Caenorhabditis elegans* is transmitted between cells by the transport of double-stranded RNA (dsRNA). The efficiency of such transmission, however, depends on both the cell type and the environment. Here, we identify systemic RNAi defective-3 (SID-3) as a conserved tyrosine kinase required for the efficient import of dsRNA. Without SID-3, cells perform RNA silencing well but import dsRNA poorly. Upon overexpression of SID-3, cells import dsRNA more efficiently than do wild-type cells and such efficient import of dsRNA requires an intact SID-3 kinase domain. The mammalian homolog of SID-3, activated cdc-42-associated kinase (ACK), acts in many signaling pathways that respond to environmental changes and is known to directly associate with endocytic vesicles, which have been implicated in dsRNA transport. Therefore, our results suggest that the SID-3/ACK tyrosine kinase acts as a regulator of RNA import into animal cells.

Intercellular signaling can occur through the transport of RNA between cells (reviewed in ref. 1). In some animals such transport occurs in response to the expression or ingestion of double-stranded RNA (dsRNA) and in plants the transport of endogenous RNAs between cells can mediate epigenetic effects during development. The import of dsRNA and mobile silencing RNA into *Caenorhabditis elegans* cells occurs via a conserved dsRNA transporter called systemic RNAi defective-1 (SID-1) (2) and mammalian homologs of SID-1 have been reported to import dsRNA into cells (3, 4). Despite this conservation of import mechanisms and the detection of the transfer of RNAs between cultured mammalian cells (5), the intercellular transport of RNA has not been robustly detected in mammals. In *C. elegans*, however, transport of silencing RNAs is easily observed from neurons, muscles, and the gut to other tissues (6). However, the efficiency of such transport varies between cell types (6) and is influenced by environmental conditions, such as starvation (2) or the presence of excess environmental dsRNA (7). Furthermore, this variation may underlie the inability to detect RNA transport between *C. elegans* cells in some studies (8, 9). Similar differences have also been reported in *Drosophila*: silencing triggered by injected dsRNA spreads throughout the fly (10) but silencing triggered by the expression of dsRNA in specific tissues does not (11). A possible explanation for this variation in the detection of RNA transport between cells is that there are mechanisms that interfere with such transport. Therefore, the identification of signaling pathways that control the efficiency of RNA transport could both enable the discovery of mechanisms that modulate RNA transport in response to the environment and enhance the reliable detection of RNA transport between cells in animals.

Results

***sid-3* Encodes the *C. elegans* Ortholog of Mammalian Activated cdc-42-Associated Kinase.** We previously used a genetic screen in *C. elegans* to identify genes that control the transport of RNA between cells (2). These systemic RNAi defective (*sid*) mutants comprise three large complementation groups: *sid-1*, *sid-2*, and *sid-3*. The *sid-1* gene encodes a conserved membrane protein with multiple transmembrane domains that imports silencing RNAs into cells (2, 6, 12, 13); *sid-2* encodes a single-pass transmembrane domain protein that is required for the import of

ingested dsRNA across the gut luminal membrane (14). In this study, we present the analysis of *sid-3*.

For the *sid* screen (2), we created a transgenic strain that allows for rapid discrimination between mutants simply defective for RNAi and mutants defective in the transport of RNA silencing signals. Animals of this strain express GFP in two tissues, the pharynx and the body wall muscle (bwm) cells, and also express *gfp*-dsRNA in the pharynx. In wild-type animals the pharyngeally expressed *gfp*-dsRNA silences pharyngeal GFP expression and, via the transport of silencing signals, also silences some anterior bwm cell GFP expression. When these animals are grown on bacteria that express *gfp*-dsRNA, then all anterior and posterior bwm cells are also silenced (Fig. 1A, Upper), making the strain suitable for large-scale phenotypic screening. In RNAi-defective mutants, silencing is not observed in any tissue, but in mutants defective in the uptake of dsRNA from the environment (e.g., *sid-2*), strong silencing of GFP expression is observed in pharyngeal and some anterior bwm cells but not in posterior bwm cells. In systemic RNAi mutants (e.g., *sid-1*) the strong silencing of pharyngeal GFP remains intact, but silencing in bwm cells, which is dependent on mobile silencing signals, is not observed. All isolated *sid-3* mutants (14 alleles) appeared similar to *sid-1* mutants in that silencing of the bwm cell GFP expression was greatly reduced but, unlike *sid-1*-null mutants, was not eliminated (Fig. 1A, Lower). In addition, GFP expression in the pharynx was to a greater extent in *sid-3*(-) animals than in wild-type animals (Fig. 1A). Taken together, our results suggest that *sid-3* mutants are defective in the transport of silencing RNAs.

We used two-factor mapping to narrow the location of the *sid-3* mutation to a small region of the *C. elegans* genome. To determine whether these recombinants were Sid, we used the highly penetrant resistance of *sid-3* mutants to feeding RNAi of GFP (Fig. 1A) or of the germ-line and embryonic gene *pal-1* (15). This mapping placed *sid-3* to the right of the visible marker *unc-3* on the X chromosome (Fig. S1A) in a region with significantly reduced recombination (16). To enable the isolation of recombinants in this region, we used a *dpy-28*(-)/*dpy-28*(+) background, which increases the crossover frequency in this region (16). Using this approach, we isolated 286 recombinants between the N2 and CB4856 polymorphic strains that had recombined to the right of *unc-3* (Fig. S1A). Analysis of these recombinants narrowed the region containing *sid-3* to the terminal 588 kb of the X chromosome (Fig. S1A). To identify DNA sequence changes within the *sid-3* region associated with the *sid-3*(*qt40*) allele, we

Author contributions: A.M.J. and C.P.H. designed research; A.M.J., Y.A.K., S.L.-E., and C.P.H. performed research; A.M.J., Y.A.K., and C.P.H. analyzed data; and A.M.J., Y.A.K., S.L.-E., and C.P.H. wrote the paper.

The authors declare no conflict of interest.

This article is a PNAS Direct Submission.

¹A.M.J. and Y.A.K. contributed equally to this work.

²Present address: Department of Cell Biology and Molecular Genetics, University of Maryland, College Park, MD 20742.

³To whom correspondence should be addressed. E-mail: Craig_Hunter@harvard.edu.

This article contains supporting information online at www.pnas.org/lookup/suppl/doi:10.1073/pnas.1201153109/-DCSupplemental.

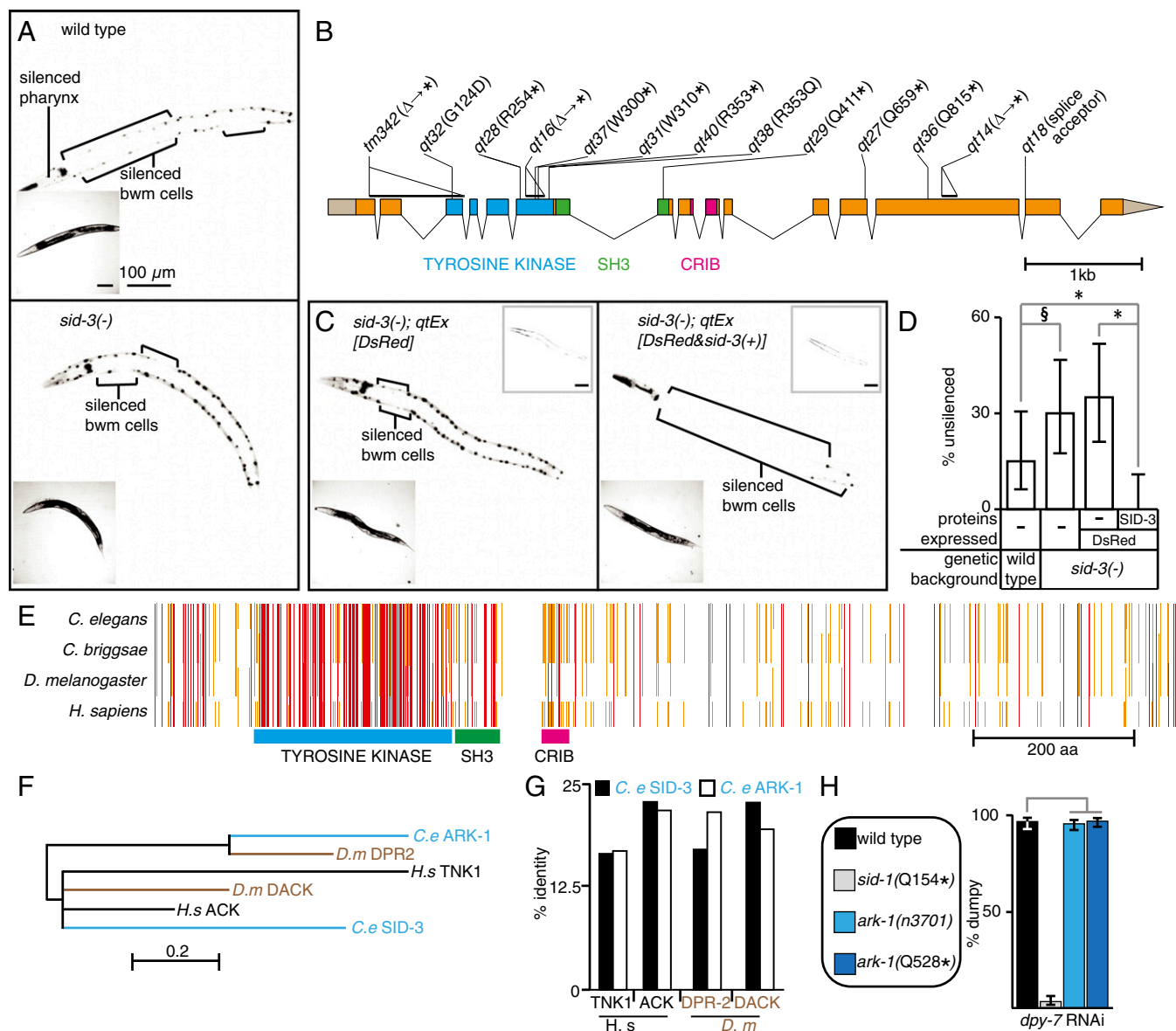


Fig. 1. *sid-3* encodes a tyrosine kinase that regulates mobile RNA silencing. (A) *sid-3(-)* animals are defective in systemic RNAi. Representative wild-type (Upper) and *sid-3(-)* (Lower) animals where GFP expression in the pharynx and bwm cells is silenced (brackets) because of both pharynx-expressed and ingested *gfp-dsRNA*. Insets are brightfield images. (B) Gene structure of *sid-3* showing mutations in isolated *sid-3(-)* alleles and the deduced changes in the SID-3 protein. Δ , deletion; *, stop codon. *sid-3(tm342)* was obtained from the *C. elegans* stock center. The tyrosine kinase domain (blue), SH3 domain (green), and CRIB domain (pink) are shown. (C) The silencing defect in *sid-3(-)* animals is rescued by *sid-3(+)* expression. Unlike expression of the fluorescent protein DsRed alone (Left, *qtEx[DsRed]*), coexpression of *sid-3(+)* (Right, *qtEx[DsRed&sid-3(+)]*) results in robust silencing in the bwm cells of *sid-3(-)* animals. Left Insets are brightfield images and Right Insets are red channel images. (D) Penetrance of silencing depicted in A and C. For each strain, the proportions of animals that lack detectable silencing are shown. Error bars indicate 95% confidence intervals. $n = 40$; * $P < 0.05$; $^{\S}P = 0.054$. (E) Schematic of multiple sequence alignment of SID-3 with its orthologs from *Caenorhabditis briggsae*, *Drosophila melanogaster*, and *Homo sapiens*. Known domains as in B and amino acid residues identical in three (orange) or in four (red) species are shown. (F) Phylogenetic relationship between the kinase domains of SID-3 and that of its paralog and homologs. Scale indicates amino acid substitution rate. (G) Similarity across the whole protein between SID-3, its paralog, and homologs in other species. SID-3 (black) shows greater identity than ARK-1 (white) to the human and fly ACK homologs. (H) *ark-1* mutants do not have a significant defect in silencing the skin gene *dpy-7* by feeding RNAi. See Fig 2 for details of the assay.

sequenced the genomic DNA from *sid-3(qt40)* animals using whole-genome sequencing (17). We identified a point mutation that results in a premature stop codon in the gene B0302.1 (Fig. S1 B and C), the exon-intron structure of which (Fig. 1B) is well supported by RNA-Seq data for each developmental stage (Fig. S2). We next sequenced DNA corresponding to the exons and exon-intron junctions of B0302.1 from 12 additional *sid-3* mutant alleles. In all, 9 of the 13 alleles had point mutations or small deletions that result in premature stop codons in the corresponding

protein; one had a splicing acceptor mutation; and two others had missense mutations that drastically altered conserved residues (Gly to Asp and Arg to Gln). (Fig. 1B and Figs. S3, S4, and S5). These observations suggest that severe disruption of the SID-3 protein is required to cause a readily detectable defect in mobile RNA silencing in our genetic screen. Confirming the gene identity of *sid-3*, we found that overexpression of genomic DNA containing B0302.1 along with its promoter and 3' UTR regions robustly rescued the silencing defect in *sid-3(-)* animals (Fig. 1C, compare Left and

Right). Interestingly, compared with wild-type animals, *sid-3(-)* animals that overexpress *sid-3(+)* showed silencing of GFP expression in a greater number of bwm cells (expressivity) and showed robust silencing in a larger fraction of the animals (penetrance) (Fig. 1D). Thus, B0302.1 encodes SID-3 and the extent of silencing because of mobile silencing RNA depends on the level of SID-3 expression.

The *sid-3* gene encodes a conserved protein with a tyrosine kinase domain, a Src homology 3 (SH3) domain, and a Cdc42/Rac interactive binding (CRIB) domain (Fig. 1B and E, and Fig. S4). This domain composition is present in the activated Cdc-42-associated kinase (Ack) family of cytoplasmic tyrosine kinases (Fig. 1E and Fig. S4) (reviewed in ref. 18). *C. elegans* contains two members of this broadly conserved family of tyrosine kinases: SID-3 and Ack related kinase-1 (ARK-1). Phylogenetic analysis suggests that the kinase domain of SID-3, rather than that of ARK-1, is more closely related to human ACK (Fig. 1F). Although both ARK-1 and SID-3 are more similar to ACK than the other human Ack-family protein TNK1 (Fig. 1G), *ark-1(-)* animals do not have a defect in silencing because of mobile RNA (Fig. 1H). To test whether ACK can rescue the silencing defects in *sid-3(-)* animals, we transformed *sid-3(-)* animals with a mouse ACK cDNA under the control of either the *sid-3* promoter or a bwm promoter (see SI Materials and Methods for details). In both cases, we failed to obtain viable transgenic lines but observed larval and embryonic lethality in the progeny of injected animals. Thus, although it remains unclear whether ACK can functionally replace SID-3 in systemic RNAi, the sequence similarity and analysis of *ark-1(-)* animals suggest that

SID-3 is the only *C. elegans* ortholog of the mammalian ACK protein with a defect in the transport of mobile RNA.

SID-3 Is Required for Efficient Feeding RNAi in all Tested Tissues and Is Localized in the Cytoplasm of Many Tissues.

To test whether *sid-3(-)* animals have defects in RNA silencing beyond the inability to silence GFP expression in bwm cells in response to mobile RNA, we examined their response to feeding RNAi of genes expressed in multiple tissues. Using two outcrossed *sid-3* null mutants [*sid-3(W310Stop)* and the *sid-3(tm342)* deletion that leads to a premature stop codon], we tested the requirement for *sid-3* to silence skin- (*dpy-7*), muscle- (*unc-22* and *unc-45*), germ line- (*par-1* and *pos-1*), and intestine-expressed (*act-5*) genes (Fig. 2A–C). In all cases, *sid-3* null mutants were measurably defective in silencing the target gene, although the severity of the defect varied among tissues and was often less penetrant than *sid-1*-null mutants (e.g., germ-line and intestinal genes). In particular, *sid-3(-)* animals were only mildly defective in silencing the intestine-expressed gene *act-5*. This observation suggested that, unlike SID-1 or SID-2, the SID-3 protein may not be required for the import of ingested dsRNA into intestinal cells but rather is required for the subsequent export of dsRNA from intestinal cells to internal tissues. Because the *sur-5::gfp* transgene expresses nuclear-localized GFP in all somatic cells, which is easily observed in the large intestinal nuclei, we measured the extent of GFP silencing in intestinal nuclei of individual *sid-3(-);sur-5::gfp* animals in response to *gfp* feeding RNAi. We found that *sid-3(-)* animals clearly showed a measurable defect in silencing GFP expression in intestinal cells, although they were more silenced than the completely defective *sid-1(-)* animals (Fig. 2D–G). In summary,

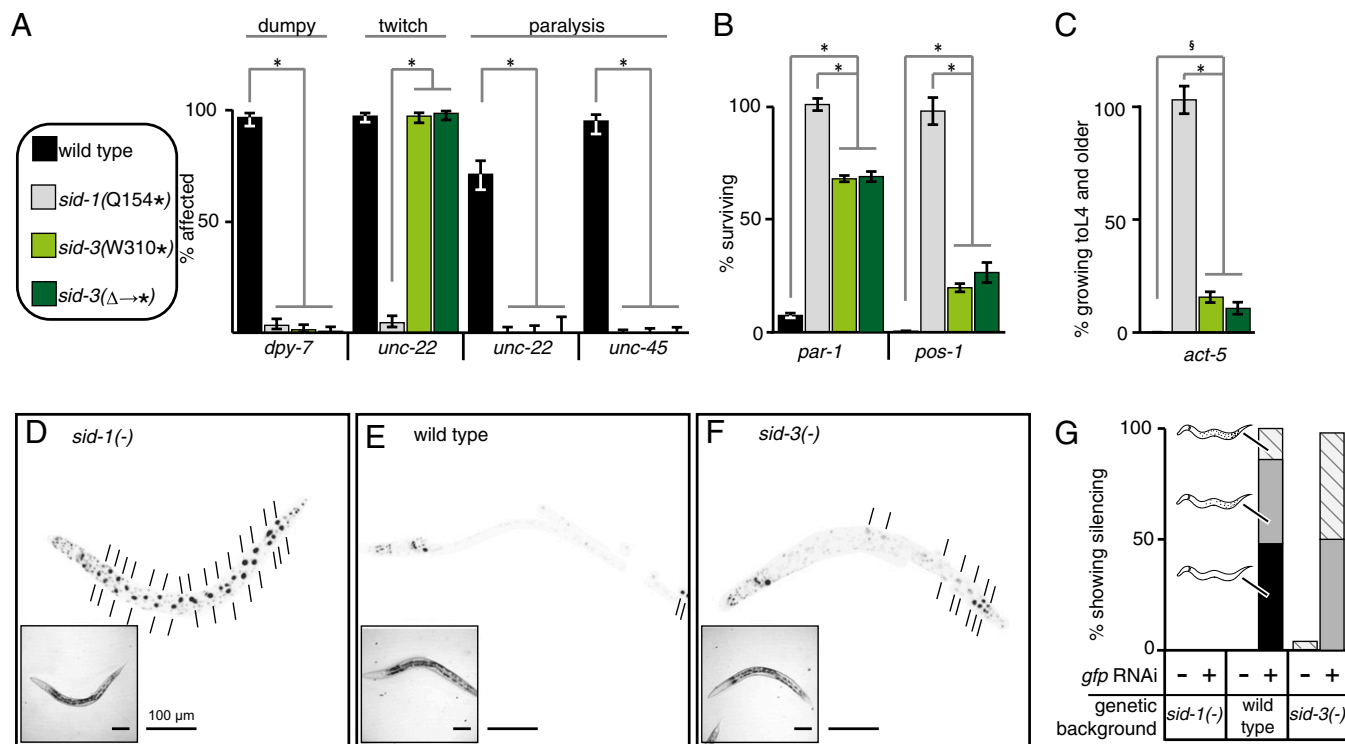


Fig. 2. *sid-3* mutants are defective for feeding RNAi in all tested tissues. (A–C) Feeding RNAi of endogenous genes. Fourth larval stage (L4) animals of wild-type, *sid-1(-)*, and two *sid-3(-)* strains with mutations that result in early stop codons [*sid-3(W310*)* and the *tm342* deletion *sid-3(Δ→*)*] were fed bacteria expressing dsRNA that target skin (*dpy-7*), muscle (*unc-22* and *unc-45*) (A), embryonic (*par-1* and *pos-1*) (B), or intestinal (*act-5*) genes (C). Percentage of affected (for skin and muscle genes) or surviving (for embryonic and intestinal genes) progeny are shown. Error bars indicate 95% confidence intervals. $n \geq 100$; * $P < 0.05$; [§]*sid-3(W310*)* vs. wild-type ($P = 0.02$) and *sid-3(Δ→*)* vs. wild-type ($P = 0.053$). (D–G) Feeding RNAi of *gfp* expression in transgenic animals. L4 animals that express GFP in all somatic nuclei (*sur-5::gfp*) in *sid-1(-)* (D), wild-type (E), or *sid-3(tm342)* (F) backgrounds were fed bacteria expressing *gfp*-dsRNA. Short lines indicate unsilenced gut nuclei (black). Proportions of progeny that show increasing extents of silencing (hatch < gray < black) are indicated along with representative schematics (G). $n = 25$ –50 worms; *insets* are brightfield images. (Scale bars, 100 μ m).

these results suggest that because SID-3 is required to fully silence genes expressed in many tissues, including intestinal cells in response to ingested dsRNA, *sid-3* is likely to function broadly to control silencing in most tissues.

To determine the tissues that express the *sid-3* gene, we constructed reporters designed to express either GFP or DsRed under the control of the *sid-3* promoter and 3' UTR regions that were used to rescue *sid-3(-)* in Fig. 1. These transcriptional reporters were expressed in multiple distinct cell types, including the gut, pharynx, bwm, skin, and excretory canal cells (Fig. 3). To examine the subcellular localization of the SID-3 protein, we generated translational reporter constructs designed to express a SID-3::DsRed fusion protein under the control of the same *sid-3* promoter and 3' UTR regions used above. The SID-3::DsRed fusion protein rescued the silencing defects in *sid-3(-)* animals (100% of animals expressing SID-3::DsRed showed silencing upon *dpy-7* feeding RNAi) and, similar to the mammalian Ack proteins (19), was localized within the cytoplasm of cells in a diffuse as well as punctate pattern in all examined tissues (Fig. 3). To ensure that the punctate localization of SID-3::DsRed was not a result of nonspecific aggregation induced by fusion to the DsRed protein, we similarly generated a SID-3::GFP fusion protein. This fusion protein was also broadly expressed and localized to the cytoplasm of cells in a diffuse as well as punctate pattern (Fig. S6).

These results suggest that the SID-3 protein likely functions in the cytoplasm of most tissues to enable efficient RNAi in response to ingested dsRNA.

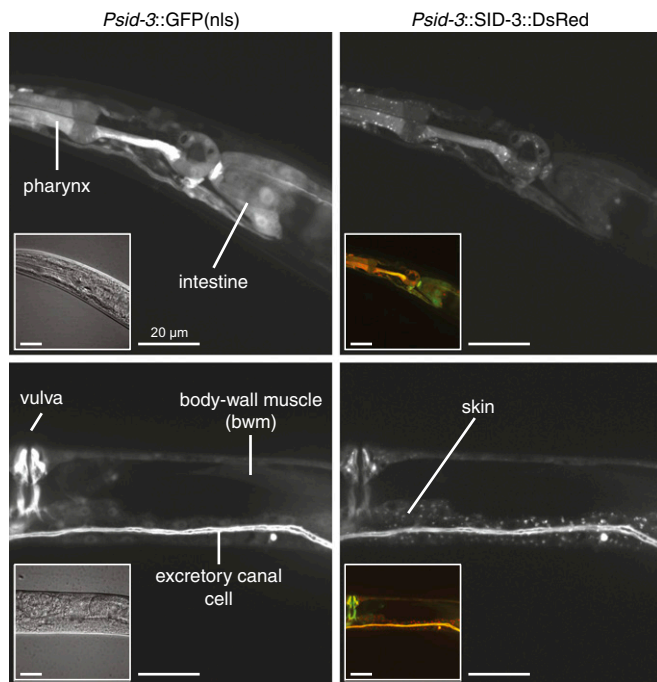


Fig. 3. SID-3 is a widely expressed cytoplasmic protein. Fluorescence images of animals that coexpress nuclear-enriched GFP (*Left*) and a rescuing SID-3::DsRed fusion protein (*Right*) under the control of the *sid-3* promoter and 3' UTR. *Left Insets* are differential interference contrast images and *Right Insets* are merged red and green channel images. Fluorescence from SID-3::DsRed was detected diffusely throughout the cytoplasm and in cytoplasmic foci. Similar diffuse and focal expression was also observed using a SID-3::GFP fusion protein (Fig. S6). Note that extrachromosomal arrays, which express the fluorescent proteins above, are lost mitotically, resulting in mosaic expression. For the more stable extrachromosomal arrays, the mosaic expression patterns largely match the known cell lineage. (Scale bars, 20 μ m.)

SID-3 Is Not Defective in Cell-Autonomous RNAi but Is Defective in the Transport of RNA Between Cells. This broad distribution of SID-3 could reflect that SID-3 is necessary for the efficient execution of RNAi (cell-autonomous RNAi) in all tissues or that SID-3 is necessary for the efficient transport of dsRNA to all tissues. The lack of a silencing defect in pharyngeal cells that express dsRNA (Fig. 1*B*) suggests that the ability to execute RNAi is not compromised in *sid-3(-)* animals. However, because the level of dsRNA expression in the pharynx is unknown, a high level of dsRNA expression in the pharynx could mask a mild defect in the execution of RNAi in *sid-3(-)* animals.

To clearly distinguish defects in the execution of RNAi from defects solely in the transport of dsRNA, we measured the response of *sid-3(-)* animals to known amounts of dsRNA injected into cells. Specifically, we injected different concentrations of dsRNA targeting an embryonic gene (*pal-1*) directly into both gonad arms of animals and measured the fraction of progeny that showed embryonic lethality (Fig. 4*A*). The germ line within the gonad is syncytial and so does not require dsRNA transport for silencing. Wild-type animals injected with increasing concentrations of *pal-1*-dsRNA laid an increasing proportion of dead progeny. The lethality was specifically caused by RNAi because no lethality was observed at any of the concentrations tested in *rde-1(-)* animals, which are resistant to RNAi. In this assay, *sid-3* mutants laid a greater proportion of dead progeny than did wild-type animals at all dsRNA doses. This finding suggests that cell-autonomous RNAi may be enhanced in *sid-3(-)* animals. To test this possibility rigorously we used a single needle containing a limiting but identical concentration (10 ng/ μ L) of *pal-1*-dsRNA to inject both gonad arms of 10 wild-type worms and 10 *sid-3(-)* worms. We then measured the proportion of dead progeny laid by each doubly injected animal (Fig. 4*B*). Although *sid-3(-)* animals appear marginally more sensitive to silencing than wild-type animals, these results were statistically indistinguishable ($P > 0.05$ Mann-Whitney U test). Nevertheless, these results clearly demonstrate that *sid-3* mutants are not defective in the execution of RNAi. Furthermore, the minor enhanced RNAi observed in response to injection of dsRNA into the germ line and the enhanced silencing of pharyngeal GFP because of *gfp*-dsRNA expression within the pharynx (Fig. 1*A*) suggest that *sid-3* mutants may even be enhanced for the execution of RNAi. Therefore, our results are consistent with the idea that the partial silencing defect in response to mobile RNA observed in *sid-3(-)* animals solely reflects a defect in RNA transport between cells.

SID-3 Is Required for the Import of Silencing RNA into Cells but Not for Their Export from Cells. SID-3 may control the export and the import of dsRNA as well as of mobile silencing RNA, which are also forms of dsRNA (20). To evaluate the roles of SID-3 in RNA transport between cells, we rescued *sid-3(-)* animals in *gfp*-dsRNA-expressing donor tissue or in GFP-expressing recipient tissue and measured silencing of GFP in the recipient tissue (Fig. 4*C* and *D*). Specifically, we used *sid-3(-)* animals that express GFP and *gfp*-dsRNA in the pharynx (donor) and that express GFP in the bwm cells (recipient). Expression of *sid-3(+)* under the control of a pharynx-specific promoter failed to rescue GFP silencing in bwm cells, suggesting that SID-3 does not have a detectable effect on the efficiency of export of mobile silencing RNA. In contrast, expression of *sid-3(+)* under the control of a bwm-specific promoter robustly rescued GFP silencing in bwm cells, suggesting that SID-3 plays a role in controlling the efficiency of mobile silencing RNA import into recipient cells. Thus, these results support the idea that SID-3 is specifically required to ensure the efficient import of mobile silencing RNA and dsRNA into *C. elegans* cells.

Tyrosine Kinase Domain of SID-3 Is Required for the Efficient Import of dsRNA into Cells. SID-3 contains several conserved protein interaction domains (Fig. 1*B*) and thus may play a structural rather

signals that activate the tyrosine kinase SID-3/ACK to promote the import of mobile silencing RNA.

Materials and Methods

Worm strains and transgenic animals were generated and maintained using standard methods (6). The position of *sid-3* was narrowed using SNP mapping and the corresponding mutation was identified using whole-genome sequencing (17). Rescues of *sid-3* mutants were performed using PCR products amplified from genomic DNA and fused with different promoter sequences. Resistance to RNAi was evaluated using feeding RNAi or injection

of dsRNA. Detailed procedures and a list of the PCR primers used are provided in *SI Materials and Methods*.

ACKNOWLEDGMENTS. We thank Marie Sutherlin (C.P.H. laboratory) for mapping data; Daniel Schott (C.P.H. laboratory) for advice on phylogeny; Siavash Karimzadegan (O. Hobert laboratory) and Christian Daly (Center for Systems Biology, Harvard University) for advice on Illumina sequencing; Robert Horvitz and members of the C.P.H. laboratory, particularly Kenneth Pang, Daniel Schott, Jacqueline Brooks, and Philip Shiu, for critical comments on the manuscript; and the *Caenorhabditis elegans* Genetics Center for some of the strains used. This work was funded in part by the National Institutes of Health (A.M.J. and C.P.H.) and the National Science Foundation (C.P.H.).

1. Melnyk CW, Molnar A, Baulcombe DC (2011) Intercellular and systemic movement of RNA silencing signals. *EMBO J* 30:3553–3563.
2. Winston WM, Molodowitch C, Hunter CP (2002) Systemic RNAi in *C. elegans* requires the putative transmembrane protein SID-1. *Science* 295:2456–2459.
3. Wolfrum C, et al. (2007) Mechanisms and optimization of in vivo delivery of lipophilic siRNAs. *Nat Biotechnol* 25:1149–1157.
4. Duxbury MS, Ashley SW, Whang EE (2005) RNA interference: A mammalian SID-1 homologue enhances siRNA uptake and gene silencing efficacy in human cells. *Biochem Biophys Res Commun* 331:459–463.
5. Valadi H, et al. (2007) Exosome-mediated transfer of mRNAs and microRNAs is a novel mechanism of genetic exchange between cells. *Nat Cell Biol* 9:654–659.
6. Jose AM, Smith JJ, Hunter CP (2009) Export of RNA silencing from *C. elegans* tissues does not require the RNA channel SID-1. *Proc Natl Acad Sci USA* 106:2283–2288.
7. Timmons L, Tabara H, Mello CC, Fire AZ (2003) Inducible systemic RNA silencing in *Caenorhabditis elegans*. *Mol Biol Cell* 14:2972–2983.
8. Tijsterman M, May RC, Simmer F, Okihara KL, Plasterk RH (2004) Genes required for systemic RNA interference in *Caenorhabditis elegans*. *Curr Biol* 14:111–116.
9. Esposito G, Di Schiavi E, Bergamasco C, Bazzicalupo P (2007) Efficient and cell specific knock-down of gene function in targeted *C. elegans* neurons. *Gene* 395:170–176.
10. Dzitoyeva S, Dimitrijevic N, Manev H (2003) Gamma-aminobutyric acid B receptor 1 mediates behavior-impairing actions of alcohol in *Drosophila*: Adult RNA interference and pharmacological evidence. *Proc Natl Acad Sci USA* 100:5485–5490.
11. Roignant JY, et al. (2003) Absence of transitive and systemic pathways allows cell-specific and isoform-specific RNAi in *Drosophila*. *RNA* 9:299–308.
12. Feinberg EH, Hunter CP (2003) Transport of dsRNA into cells by the transmembrane protein SID-1. *Science* 301:1545–1547.
13. Shih JD, Hunter CP (2011) SID-1 is a dsRNA-selective dsRNA-gated channel. *RNA* 17:1057–1065.
14. Winston WM, Sutherlin M, Wright AJ, Feinberg EH, Hunter CP (2007) *Caenorhabditis elegans* SID-2 is required for environmental RNA interference. *Proc Natl Acad Sci USA* 104:10565–10570.
15. Hunter CP, Kenyon C (1996) Spatial and temporal controls target *pal-1* blastomere-specification activity to a single blastomere lineage in *C. elegans* embryos. *Cell* 87:217–226.
16. Tsai CJ, et al. (2008) Meiotic crossover number and distribution are regulated by a dosage compensation protein that resembles a condensin subunit. *Genes Dev* 22:194–211.
17. Sarin S, Prabhu S, O'Meara MM, Pe'er I, Hobert O (2008) *Caenorhabditis elegans* mutant allele identification by whole-genome sequencing. *Nat Methods* 5:865–867.
18. Prieto-Echagüe V, Miller WT (2011) Regulation of ack-family nonreceptor tyrosine kinases. *J Signal Transduct* 2011:742372.
19. Grøvdal LM, Johannessen LE, Rodland MS, Madshus IH, Stang E (2008) Dysregulation of Ack1 inhibits down-regulation of the EGF receptor. *Exp Cell Res* 314:1292–1300.
20. Jose AM, Garcia GA, Hunter CP (2011) Two classes of silencing RNAs move between *Caenorhabditis elegans* tissues. *Nat Struct Mol Biol* 18:1184–1188.
21. Loughheed JC, Chen R-H, Mak P, Stout TJ (2004) Crystal structures of the phosphorylated and unphosphorylated kinase domains of the Cdc42-associated tyrosine kinase ACK1. *J Biol Chem* 279:44039–44045.
22. Yokoyama N, Miller WT (2003) Biochemical properties of the Cdc42-associated tyrosine kinase ACK1. Substrate specificity, autophosphorylation, and interaction with Hck. *J Biol Chem* 278:47713–47723.
23. Manser E, Leung T, Salihuddin H, Tan L, Lim L (1993) A non-receptor tyrosine kinase that inhibits the GTPase activity of p21cdc42. *Nature* 363:364–367.
24. Harris KP, Tepass U (2010) Cdc42 and vesicle trafficking in polarized cells. *Traffic* 11:1272–1279.
25. Saleh MC, et al. (2006) The endocytic pathway mediates cell entry of dsRNA to induce RNAi silencing. *Nat Cell Biol* 8:793–802.
26. Shen H, et al. (2011) Constitutive activated Cdc42-associated kinase (Ack) phosphorylation at arrested endocytic clathrin-coated pits of cells that lack dynamin. *Mol Biol Cell* 22:493–502.
27. Zielinska DF, Gnäd F, Jedrusik-Bode M, Wiśniewski JR, Mann M (2009) *Caenorhabditis elegans* has a phosphoproteome atypical for metazoans that is enriched in developmental and sex determination proteins. *J Proteome Res* 8:4039–4049.
28. Galisteo ML, Yang Y, Ureña J, Schlessinger J (2006) Activation of the nonreceptor protein tyrosine kinase Ack by multiple extracellular stimuli. *Proc Natl Acad Sci USA* 103:9796–9801.

Supporting Information

Jose et al. 10.1073/pnas.1201153109

SI Materials and Methods

Strains Used. N2 Bristol wild-type (used in all experiments except mapping), CB4856 Hawaiian wild-type, HC57 *qtIs3(Pmyo2::gfp/hpRNA);mIs11(Pmyo2::GFP);ccIs4251(Pmyo3::GFP)* (1), HC114 *qtIs3;mIs11;ccIs4251;sid-1(qt9)* (1), HC115 *ccIs4251;unc-6(e78) dpy-6(e14) sid-3(qt14)*, HC111 *qtIs3;mIs11;ccIs4251;sid-3(qt11)*, HC118 *qtIs3;mIs11;ccIs4251;sid-3(qt16)*, HC120 *qtIs3;mIs11;ccIs4251;sid-3(qt18)*, HC152 *qtIs3;mIs11;ccIs4251;sid-3(qt27)*, HC153 *qtIs3;mIs11;ccIs4251;sid-3(qt28)*, HC154 *qtIs3;mIs11;ccIs4251;sid-3(qt29)*, HC156 *qtIs3;mIs11;ccIs4251;sid-3(qt31)*, HC157 *qtIs3;mIs11;ccIs4251;sid-3(qt32)*, HC161 *qtIs3;mIs11;ccIs4251;sid-3(qt36)*, HC162 *qtIs3;mIs11;ccIs4251;sid-3(qt37)*, HC163 *qtIs3;mIs11;ccIs4251;sid-3(qt38)*, HC164 *qtIs3;mIs11;ccIs4251;sid-3(qt39)*, HC165 *qtIs3;mIs11;ccIs4251;sid-3(qt40)*, HC195 *nrls20[sur-5::gfp]*, HC196 *sid-1(qt9)*, HC566 *nrls20;sid-1(qt9)*, HC769 *sid-3(qt31)* [outcrossed twice to N2], HC770 *sid-3(tm342)* [outcrossed twice to N2], HC771 *nrls20;sid-3(tm342)*, MT11836 *ark-1(n3701)*, PS1461 *ark-1(sy247)*, WM27 *rde-1(ne219)*, and TY148 *dpy-28(y1)*.

SNP Mapping. Two-factor mapping indicated that *sid-3* is located in a region of recombination suppression to the right of *unc-3* on the X chromosome (2). Specifically, using the *sid-3(qt40)* allele, we found that 9/9 *Dpy-6-non-Unc-3* were systemic RNAi defective (Sid) (as evidenced by resistance to *pal-1* feeding RNAi) and 28/28 *Unc-3-non-Dpy-6* animals were non-Sid (as evidenced by sensitivity to *pal-1* feeding RNAi). A *dpy-28(-)/dpy-28(+)* background was used to increase recombination in this region (2). HC115 was crossed into a strain that was Hawaiian on the X chromosome but that had *dpy-28(y1)* in the background and recombinants that separate *unc-6* and *dpy-6* from *sid-3* were isolated. These recombinants were tested for the following SNPs between the Bristol and Hawaiian strains: *pkP6167*, *pkP6168*, *pkP6169*, *pkP6170*, *pkP6171*, and *pkP6172*, *haw111990*, and *CE6-243*. The SNPs were identified using primers as listed in wormbase (www.wormbase.org) and either restriction enzyme digests or Sanger sequencing. Using this approach, 286 recombinants were analyzed to position *sid-3* to the terminal ~588-kb region after *haw111990* on the X chromosome.

Outcross and Genotyping. The *sid-3(qt31)* mutation was isolated from the GFP and *gfp-pfjg* hpRNA transgenes by backcrossing HC156 with N2 twice. Successful backcrosses were identified by the lack of GFP expression and restriction fragment length polymorphisms. The region containing the point mutation (*qt31*) was amplified through PCR with primers P55 and P56, and then cut with the enzyme *NcoI*, which cuts wild type but not the mutant. *sid-3(tm342)* was made from heterozygotes of a deletion in B0302.1, *tm342* (National Bioresource Project for the nematode and Shohei Mitani, Department of Physiology, Tokyo Women's Medical University School of Medicine, Tokyo, Japan), by backcrossing with N2 twice. The deletion was followed using a set of primers (P51, P52, P54) that yielded different length PCR fragments for wild-type and the deletion.

Preparation of Sample for Whole-Genome Sequencing and Verification by T/A Cloning. HC165 genomic DNA was purified to eliminate RNA using a protocol adapted from Qiagen Puregene Core Kit and the Hobert Laboratory (3), and the DNA concentration was measured using a NanoDrop spectrophotometer. Next, 1.5 μ g of the DNA (406.4 ng/ μ L) was fragmented for 20 min with Fragmentase (New England Biolabs). End repair, addition of a 3' A, and ligation of Illumina adapters were done as per the protocol

from Illumina (3). The resultant library was then run on a 2% (wt/vol) agarose gel and bands from 100 to 250 bp were excised and purified using Gel Extraction Kit (Qiagen) and MinElute PCR Purification Kit (Qiagen). The library was amplified using Illumina primers complementary to the adapter sequences. The final concentration of the library was 19.5 ng/ μ L. Using the StrataClone PCR Cloning Kit (Stratagene), DNA from the library was inserted into plasmids with LacZ and ampicillin resistance through TA TOPO cloning. StrataClone competent cells were transformed with the plasmid and grown on Luria broth plates with 100 μ g/mL of carbenicillin for blue/white color screening. White or light blue colonies were picked and the inserts were Sanger-sequenced. Thirteen of the 15 distinct insert sequences obtained mapped to the *Caenorhabditis elegans* genome and two mapped to the *Escherichia coli* genome (likely from contaminating food). Because a majority of the sequences were from HC165, we proceeded with this library for whole-genome sequencing.

Bioinformatic Analysis After Whole-Genome Sequencing. We obtained 22,005,912 reads that were each 42 bases long from sequencing (Illumina GAI system). We used Galaxy (4–6) to analyze and align the reads to the *C. elegans* genome (ce6). These Illumina reads were entered into Galaxy and 21.7 million reads of good quality were culled (quality score ≥ 10 and maximum number of bases allowed outside of quality for each read was 3). As 3' ends were more variable in quality, we trimmed three bases off the 3' ends to increase alignment fidelity. Upon alignment, 81% of the reads (i.e., 17,583,185 reads with a read length of 39 bases) mapped to the *C. elegans* genome for a 6.85 \times coverage of the genome. Of the mapped reads, we filtered for reads on the X chromosome to the right of *haw111990*, leaving 472,865 reads. From these reads, we filtered for candidate mutations (covered by at least one read and with more than half the reads different from the reference sequence) to obtain 32 candidates.

Testing the Candidate Mutations. Regions containing each of the candidate mutations were amplified by PCR using 25 sets of primers (P1–P50). The PCR products were purified using Qiagen PCR Column Purification and Sanger-sequenced. Nine of these products were successfully sequenced and three of the nine (one in an exon, two in introns) were confirmed as true mutations. The remaining six were false-positives from Illumina sequencing that did not reconfirm by Sanger sequencing. Unlike the false-positives, the three mutations confirmed were strong candidates as all of the Illumina reads that covered the corresponding base had the mutation.

Sequencing the Other Alleles of *sid-3*. To find the mutations in the 12 remaining alleles of *sid-3* other than *qt40* (used for Illumina sequencing) and *tm342* (known deletion), we designed primers (P51–P70) to sequence all of the known exons of B0302.1 according to Wormbase and confirmed by the modENCODE project (Fig. S2). Parts of the gene that contain exons were amplified by PCR (Fig. S3) and the PCR products were then purified using PCR Column Purification kit (Qiagen) and Sanger-sequenced.

DNA Constructs and Transgenesis. Coinjection markers. The plasmids pRF4 (7), pHC183 (1), and pHC448 (8) were used to obtain transgenic animals that roll, express DsRed2 in the body wall muscles (bwm), or express DsRed2 in the pharynx, respectively. **PCR fusion products.** Except as noted, promoter, gene, and 3' UTR sequences were amplified from genomic DNA or plasmid

sources with PfuUltraII Fusion Polymerase (Agilent) by using primers that result in a ~50 bp overlap between the two PCR fragments. The fusion products, along with specified coding and noncoding sequences, were generated with expand long template (ELT) polymerase (Roche) by using nested primers along with the amplified promoter and the coding sequences as template. In some cases, the two or three PCR fragments were fused in vivo. The specific templates and primers used to generate the various PCR fusion products are detailed below.

To rescue *sid-3*. The entire *sid-3* gene plus 6 kb of its upstream promoter region and 450 bp of its 3' UTR was amplified using the ELT PCR system (Roche) with primers P71 and P72. Two overlapping 10-kb fragments that span the 13-kb region containing *sid-3* was used as template to amplify *sid-3* for Fig. 1. In all other cases, N2 genomic DNA was used as template to amplify *sid-3* sequences. The amplified DNA (10 ng/μL) and pHC183 (38 ng/μL) was injected into HC156 and HC769 to generate a transgenic line.

To express *sid-3* in the pharynx (*Pmyo2::sid-3* gDNA and 3' UTR). The *myo-2* promoter was amplified from pHC168 with primers P73 and P74. *Sid-3* with its 3' UTR was amplified from N2 gDNA using ELT polymerase with primers P75 and P76. The fusion product was generated with primers P73 and P77. A 1:4 mix of *Pmyo2::sid-3* gDNA and 3' UTR (10.5 ng/μL) and the coinjection marker pHC448 (38 ng/μL) was injected into HC769 animals to generate transgenic lines.

To express *sid-3* in the body wall muscles (*Pmyo3::sid-3* gDNA and 3' UTR). The *myo-3* promoter was amplified from pHC183 with primers P77 and P78. *Sid-3* with its 3' UTR was amplified from gDNA using ELT polymerase with primers P79 and P76. The fusion product was generated with primers P77 and P82. A 1:4 mix of *Pmyo-3::sid-3* gDNA and 3' UTR (10.8 ng/μL) and pHC183 (45 ng/μL) was injected into HC769 animals to generate transgenic lines.

To produce a transcriptional reporter of *sid-3* expression with GFP (*Psid-3::gfp::sid-3* 3' UTR). The 3' UTR of *sid-3* was amplified from gDNA with primers P81 and P76. The *gfp* coding sequence was amplified from pJM46a using primers P82 and P83. The fusion product *gfp::sid-3* 3' UTR was generated with primers P84 and P85. The *sid-3* promoter was amplified from gDNA using ELT polymerase and with primers P86 and P87. The final fusion product *Psid-3::gfp::sid-3* 3' UTR was generated with primers P71 and P77. A 1:4 mix of *Psid-3::gfp::sid-3* 3' UTR (10.35 ng/μL) and the coinjection marker pRF4 (44 ng/μL) was injected into HC769 animals to generate transgenic lines.

To produce a transcriptional reporter of *sid-3* localization with DsRed2 (*Psid-3::DsRed2::sid-3* 3' UTR). The 3' UTR of *sid-3* was amplified from gDNA with primers P88 and P76. The *DsRed2* coding sequence was amplified from pHC183 using primers P82 and P89. The fusion product *DsRed2::sid-3* 3' UTR was generated with primers P90 and P84. The *sid-3* promoter was amplified from gDNA using ELT polymerase and with primers P86 and P91. The final fusion product *Psid-3::DsRed2::sid-3* 3' UTR was generated with primers P71 and P77. A 1:4 mix of *Psid-3::DsRed2::sid-3* 3' UTR (10 ng/μL) and the coinjection marker pRF4 (44 ng/μL) was injected into HC769 animals to generate transgenic lines.

To express a translational fusion of *sid-3* with DsRed2 (*Psid-3::sid-3* gDNA::DsRed2::sid-3 3' UTR). The *sid-3* 3' UTR was amplified from gDNA with primers P88 and P76. The *DsRed2* coding sequence was amplified from pHC183 with primers P82 and P89. The fusion product *gfp::sid-3* 3' UTR was generated with primers P90 and P84. The *sid-3* promoter along with *sid-3* was amplified from gDNA with primers P86 and P92. The final fusion product, *Psid-3::sid-3::DsRed2::sid-3* 3' UTR, was generated with primers P71 and P77. A 1:1 mix of *Psid-3::sid-3::DsRed2::sid-3* 3' UTR (16.65 ng/μL) and the coinjection marker *Psid-3::gfp::sid-3* 3' UTR (10.35 ng/μL) was injected into HC769 animals to generate transgenic lines.

To express *sid-3(KD-)* in *bwm* cells. The *myo-3* promoter was amplified from pHC183 with primers P93 and P94 using Phusion polymerase mix. The *sid-3* coding sequence up to the kinase domain was amplified from wild-type gDNA with primers P95 and P96 using Phusion polymerase mix. The remainder of the *sid-3* gene including the 3' UTR was amplified using P97 and P98 from wild-type gDNA with ELT polymerase. An equimolar mix of *Pmyo-3* (3.8 ng/μL), *sid-3* up to kinase domain (4 ng/μL), *sid-3* from kinase domain to 3' UTR (14.6 ng/μL) was injected into HC156 animals along with the coinjection marker pHC183 (20 ng/μL) to generate transgenic lines. This construct is expected to express SID-3(K139A), a kinase-dead version of SID-3.

To express *sid-3(+)* in *bwm* cells as control for *sid-3(KD-)* expression. The *myo-3* promoter was amplified from pHC183 with primers P93 and P94 using Phusion polymerase mix (New England Biolabs). The *sid-3* coding sequence up to the kinase domain was amplified from wild-type gDNA with primers P95 and P99 using Phusion polymerase mix. The remainder of the *sid-3* gene including the 3' UTR was amplified using P100 and P98 from wild-type gDNA with ELT polymerase. An equimolar mix of *Pmyo-3* (3.8 ng/μL), *sid-3* up to kinase domain (4 ng/μL), *sid-3* from kinase domain to 3' UTR (14.6 ng/μL) was injected into HC156 animals along with the coinjection marker pHC183 (20 ng/μL) to generate transgenic lines.

To express mouse activated *cdc-42*-associated kinase in *bwm* cells. The *myo-3* promoter was amplified from pHC183 with primers P101 and P102 using Phusion polymerase mix. The activated *cdc-42*-associated kinase (*ack*) cDNA was amplified from pYX-Asc +TNK2 (Source Bioscience) with primers P103 and P104 using Phusion polymerase mix. The *unc-54* 3' UTR was amplified using P105 and P106 using Phusion polymerase from pHC183. An equimolar mix of *Pmyo-3* (4 ng/μL), *ack* cDNA (4 ng/μL), and *unc-54* 3' UTR (14.6 ng/μL) was injected into HC156 animals along with the coinjection marker pHC183 (20 ng/μL) to generate transgenic lines.

To express ACK under the control of the *sid-3* promoter as a translational fusion in *C. elegans* (*Psid-3::ack::gfp::sid-3* 3' UTR). The *sid-3* 3' UTR was amplified from gDNA with primers P107 and P108. The *gfp* coding sequence was amplified from pPD95.75 with primers P109 and P110. The fusion product *gfp::sid-3* 3' UTR was generated with primers P111 and P112. This fusion product, the *sid-3* promoter, amplified from gDNA, and ACK-1 cDNA were injected along with the coinjection marker pHC183 into HC769 animals to generate transgenic lines where the PCR products would be fused in vivo.

To express a translational fusion of *sid-3* with *gfp* (*Psid-3::sid-3* gDNA::gfp::sid-3 3' UTR). The *gfp* coding sequence was amplified from pPD95.75 with primers P113 and P114 using Phusion polymerase mix (New England Biolabs). The *sid-3* 3' UTR was amplified from gDNA with primers P115 and P116 using Phusion polymerase mix. The *sid-3* promoter along with *sid-3* was amplified from gDNA with primers P117 and P118 using ELT polymerase. An equimolar mix of *Psid-3::gfp::sid-3* (20 ng/μL), GFP (1.5 ng/μL), and *sid-3* 3' UTR (1 ng/μL) along with the coinjection marker pRF4 (20 ng/μL) was injected into HC769 animals to generate transgenic lines where the PCR products would be fused in vivo.

In most cases, transgenic animals were healthy and appeared morphologically normal, with the following exceptions. The attempt to express mouse ACK in *C. elegans* resulted in embryonic and larval lethality in the progeny of injected animals. Overexpression of wild-type *sid-3(+)* in body-wall muscles or under the control of its own promoter using in vivo fusion as above resulted in many transgenic animals with vulval, egg-laying, and movement defects.

Feeding RNAi of Endogenous Genes. *E. coli* expressing either dsRNA targeting a particular *C. elegans* gene (Geneservice) or

control dsRNA (L4440) was fed to L4-staged animals on agar plates containing 1 mM isopropyl β -D-1-thiogalactopyranoside. Progeny of these animals were examined for the corresponding defects. To measure brood size for *pal-1* and *pos-1* RNAi, three plates containing three L4 animals each were fed either RNAi food or control food and the animals moved to a new plate of the corresponding food after 2 d. All hatched progeny on the first plate were counted 2 d later (on day 4) and all hatched progeny on the second plate were counted 2 d after that (on day 6). The average brood size of the three plates of control food was used to normalize the brood size on each of the three RNAi food plates. For *act-5*, progeny of stage L4 and older were similarly counted and normalized. For *dpy-7*, the percentage of young adult progeny that were dumpy was calculated. Only those that were strongly dumpy were counted as dumpy. None of the control RNAi food plates showed any dumpy progeny. For *unc-22*, we counted percentages of L4 larvae that twitched and adults that were paralyzed. Worms unable to move upon tapping the plate were scored as paralyzed. For *unc-45*, the percentage of paralyzed L4 progeny was determined.

***gfp*-Feeding RNAi.** For *gfp* feeding RNAi, *E. coli* that expresses *gfp-hp*RNA (hairpin RNA) from the plasmid pPD126.25 was put onto nematode growth (NG) plates (3 g NaCl, 17 g agar, 2.5 g peptone, 1 mM CaCl₂, 5 mg of cholesterol, 1 mM MgSO₄, 25 mM KPO₄ in 1 L of H₂O) and three L4 worms were placed on the *E. coli* (9). OP50 on NG plates was used as control. After 4 d, 25 or 50 L4 progeny were picked under white light (for unbiased picking) and put on a new plate. These L4 progeny were then scored for GFP silencing using a dissecting fluorescent microscope at a fixed magnification.

Injection RNAi of *pal-1*. We used T7 RNA polymerase to transcribe in vitro dsRNA that targets the *pal-1* gene. A PCR product amplified from genomic DNA with dual T7 primers was used as a template to generate dsRNA. The transcribed RNA was annealed and quantified using a spectrophotometer (NanoDrop). In Fig. 4A, different concentrations of dsRNA were injected into both gonad arms of three young adult animals (24 h after L4) for each genotype and the proportion of dead progeny among progeny laid 12 h after injection was counted. In Fig. 4B, 10 ng/ μ L of dsRNA was injected into both gonads of 10 wild-type and 10 *sid-3(qt31)* animals using the same needle and alternating between the two genotypes. The proportion of dead embryos among progeny laid within a 60-h period beginning 12 h after injection was determined for each injected animal.

Phylogeny. The amino acid sequences of the kinase domains of the two Ack family proteins from *C. elegans* (SID-3 114–363 aa and ARK-1 120–376 aa), *D. melanogaster* (DACK 130–383 aa and DPR2 140–396 aa), and *H. sapiens* (ACK 196–148 aa and TNK1 123–377 aa) were used for phylogenetic analysis. The phylogeny tree was manually compiled using MUSCLE, Gblocks, PhyML, and TreeDyn at Phylogeny.fr (10). Branches with a bootstrap value <95% were collapsed to generate the final tree. The tree was arbitrarily rooted to the single resolved internode.

Statistics. The 95% confidence intervals for *dpy-7*, *unc-22*, *unc-45* feeding were calculated from Wilson's estimates with continuity correction (11). The 95% confidence intervals for *pal-1*, *pos-1*, *act-5* feeding were calculated using the Student *t* test. Significance of differences in the *pal-1* dsRNA injection experiments were assessed using the Mann–Whitney *U* test.

Live Microscopy. Worms were immobilized using 3 mM levamisole (Sigma-Aldrich) for imaging. All microscopy images are projections of Z-series made with a Zeiss spinning disk confocal microscope. Images being compared in each figure were taken

using the same nonsaturating exposure conditions and processed identically (except where indicated otherwise) using Adobe Photoshop for display.

Primers.

P1: ggctctttcacgttactttag
 P2: gttgtcttaaacgtcaacgtc
 P3: caactctcgggtttacagc
 P4: cttctcgggtttacagcgg
 P5: catttggcgaggagccatg
 P6: cccctttgtcaattgtagt
 P7: gaactgcataatctcgcgg
 P8: caagtttgcagagaaacaac
 P9: caatagttcggcattgctgg
 P10: ctacaccgactacccaac
 P11: cttttgcatgcccggatc
 P12: ccacaaaatttcagcggcg
 P13: ctcaagtggagtttttggac
 P14: gtggcttcttcttagagc
 P15: ggcgagcactttgaactgg
 P16: gtcttgggtcaaccgctc
 P17: ctgtgaaaaatattttggcggg
 P18: gaaagtcttgaacattccag
 P19: caatgagaatgctccaagg
 P20: ggcagtaatacacaagcacc
 P21: cttcagtagcacagaaagc
 P22: ctctctgtctactcgaac
 P23: gtacgacagaaagcactctg
 P24: gttctctgttactcgaag
 P25: cttcagtagcacagagaaac
 P26: cgaagtgttctgtctgtac
 P27: gtacgacagaaagcactctg
 P28: ctgttgtactcgaagcagtg
 P29: cactgcttcgagtacaacag
 P30: ctttctgtctactcgaagc
 P31: gcttcgtagcacagaaagc
 P32: gaggtaagtgctctctgtg
 P33: gcttcgtagcacagaaagc
 P34: ctgtctactcgaacagtg
 P35: ccttcaaatggtttcagcgc
 P36: cagacgtaagtagtcataggg
 P37: gcggcatggtttgttaac
 P38: cagttcaagacagtttgggtg
 P39: gtgtcttctctactgatg
 P40: cggcacagactaaactatgc
 P41: gcgctaccaataagctaagc
 P42: gaaaacattgtcaccttaattg
 P43: ggctatgcgacaaatggttg
 P44: caatgagcacttggacctg
 P45: gaaggaaacactggattagcc
 P46: gcaaattccatttgcgtccc
 P47: ctaaagaaatgagggtggatg
 P48: cagttgtgcatccaatcagg
 P49: catgttcccatttgtatgg
 P50: gttttcgtattgctgctctg
 P51: ctacgggttaaaaaaccagctc
 P52: gctctagtatgcacaaaaaac
 P53: ccaaaacacatcgtttcacc
 P54: ggacttctttttgtggagcc
 P55: gtggcagcaagggaatattttg
 P56: gctctgtcatttaaggcgcac
 P57: gagacctccttgtttttgg
 P58: gtgaccggtatggatgaaag
 P59: gaaaactcgcgtaacgacc
 P60: gggcctataaatttctctcgc
 P61: cattgaatccacccttctg
 P62: gattacgctgtcattgctctg

P63: gtgctcattccaactaaccc
 P64: gtgggtgccacattactatg
 P65: ccgtcaaatgggtfcaatgc
 P66: catttaactgagggtagccg
 P67: ggcaaaaccagtgaactcaac
 P68: gtggttcaccacgtctcg
 P69: gtcgatagcagcaatctctg
 P70: ctagtataaatggcgacgggc
 P71: ctgaaaggagcaacaagcag
 P72: ccggctactttttggtcac
 P73: cgaggcatttgaattggggg
 P74: ccctgacgtgcttgcattccgaatcgataggatctcgg
 P75: ccgagatcctatcgattcggatggcaagcacgtcagggg
 P76: ccagcaaagagagattgctc
 P77: gtgacaaaaaagtagccgg
 P78: caggctcggctataataatgctc
 P79: ccctgacgtgcttgcattgggtgacgacgggtggatc
 P80: gatccaccggtcgccaccatggcaagcacgtcagggg
 P81: ggcatggatgaactatacaaataggccaagaaactaatgtattatag
 P82: cttttcaggaggaccttg
 P83: ctataatacattagtcttctggcctattgtatagttcatccatgc
 P84: tcacttccctgtgaaggtc
 P85: ctgccattttcagacgtagcaatgagtaaaggagaagaacttttc
 P86: ttgatgtgcaagccatctgg
 P87: gaaaagtcttctctttactcattgctacgtctgaaaatggcag
 P88: ccaccacctgttctgttagggccaagaaactaatgtattatag
 P89: ctataatacattagtcttctggcctacaggaacaggtggtgg
 P90: ctgccattttcagacgtagcaatggcctcctccgagaac

P91: cgttctcggaggaggccattgctacgtctgaaaatggcag
 P92: cgttctcggaggaggccatgccgagcaacatgttggcg
 P93: cattccactacgtcatagttc
 P94: ccctgacgtgcttgcattgggtggcgaccgggtggatc
 P95: gatccaccggtcgccaccatggcaagcacgtcagggg
 P96: cgcattgtaattgctgctgcaatctccgcgacatttctcc
 P97: ggagaaatgctcgggagaattgacagcagcattcacatgcg
 P98: ccagcaaagagagattgctc
 P99: cgcattgtaattgctgctgcaaaattctccgcgacatttctcc
 P100: ggagaaatgctcgggagaatttgacagcagcattcacatgcg
 P101: cattccactacgtcatagttc
 P102: tcctcctcgggtgctgattgggtggcgaccgggtggatc
 P103: gatccaccggtcgccaccatggcaagcacgtcagggg
 P104: tcgaacgctcgggctgacgctgttggatgagcag
 P105: ctgctcatcaaaacgctgacggcccgaagggctgca
 P106: ctgaaacgtaacatagataagg
 P107: ggcatggatgaactatacaaataggccaagaaactaatgtattatag
 P108: ccagcaaagagagattgctc
 P109: cttttcaggaggaccttg
 P110: ctataatacattagtcttctggcctattgtatagttcatccatgc
 P111: tcacttccctgtgaaggtc
 P112: ctgccattttcagacgtagcaatgagtaaaggagaagaacttttc
 P113: ctataatacattagtcttctggcctattgtatagttcatccatgc
 P114: cgccaacatgttctcggcatgagtaaaggagaagaacttttc
 P115: ccagcaaagagagattgctc
 P116: ggcatggatgaactatacaaataggccaagaaactaatgtattatag
 P117: ttgatgtgcaagccatctgg
 P118: gaaaagtcttctctttactcattgctacgcaacatgttggcg

1. Winston WM, Molodowitch C, Hunter CP (2002) Systemic RNAi in *C. elegans* requires the putative transmembrane protein SID-1. *Science* 295:2456–2459.
2. Tsai CJ, et al. (2008) Meiotic crossover number and distribution are regulated by a dosage compensation protein that resembles a condensin subunit. *Genes Dev* 22:194–211.
3. Sarin S, Prabhu S, O'Meara MM, Pe'er I, Hobert O (2008) *Caenorhabditis elegans* mutant allele identification by whole-genome sequencing. *Nat Methods* 5:865–867.
4. Giardine B, et al. (2005) Galaxy: A platform for interactive large-scale genome analysis. *Genome Res* 15:1451–1455.
5. Goecks J, Nekrutenko A, Taylor J; Galaxy Team (2010) Galaxy: A comprehensive approach for supporting accessible, reproducible, and transparent computational research in the life sciences. *Genome Biol* 11:R86.
6. Blankenberg D, et al. (2010) Galaxy: A web-based genome analysis tool for experimentalists. *Curr Protoc Mol Biol* 19:10.1–10.21.
7. Mello CC, Kramer JM, Stinchcomb D, Ambros V (1991) Efficient gene transfer in *C. elegans*: Extrachromosomal maintenance and integration of transforming sequences. *EMBO J* 10:3959–3970.
8. Jose AM, Garcia GA, Hunter CP (2011) Two classes of silencing RNAs move between *Caenorhabditis elegans* tissues. *Nat Struct Mol Biol* 18:1184–1188.
9. Jose AM, Smith JJ, Hunter CP (2009) Export of RNA silencing from *C. elegans* tissues does not require the RNA channel SID-1. *Proc Natl Acad Sci USA* 106:2283–2288.
10. Dereeper A, et al. (2008) Phylogeny.fr: robust phylogenetic analysis for the non-specialist. *Nucleic Acids Res* 36(Web Server issue):W465–W469.
11. Newcombe RG (1998) Two-sided confidence intervals for the single proportion: Comparison of seven methods. *Stat Med* 17:857–872.

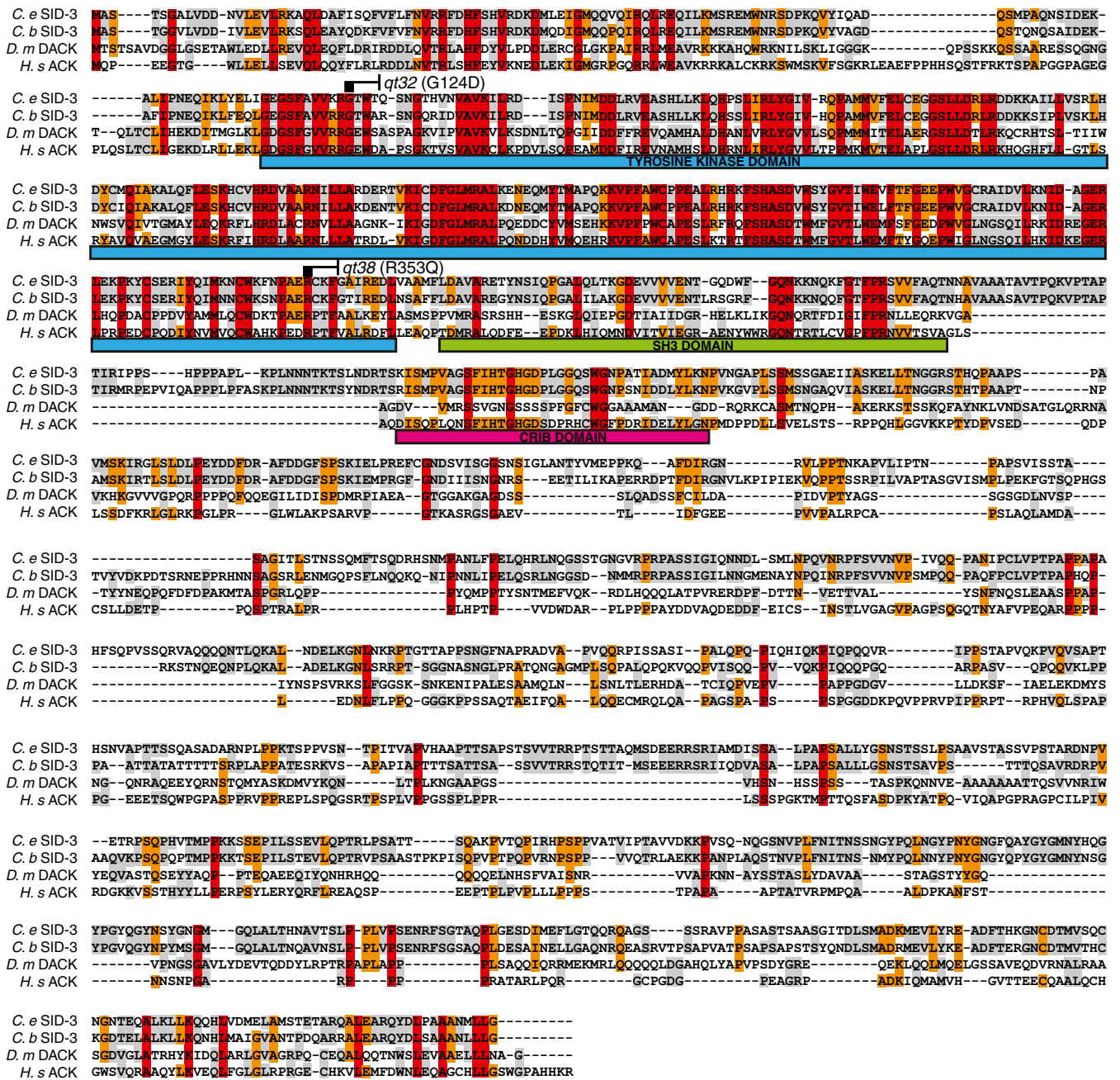


Fig. 54. SID-3 is the closest *C. elegans* homolog of human ACK. Sequence alignment between SID-3 and its closest homologs in humans (*H.s* ACK), flies (*D.m* DACK), and *Caenorhabditis briggsae* (*C.b* SID-3). Conserved domains [Tyrosine kinase domain, Src homology 3 (SH3) domain, and Cdc42/Rac interactive binding (CRIB) domain] are indicated below the alignment and changes caused by missense mutations are indicated above the alignment. Residues identical in four (red), three (orange), or two (gray) sequences are shaded in the alignment.

